Journal of Physics: Conference Series

PAPER • **OPEN ACCESS**

First-principles calculation of hot carriers in black phosphorus

To cite this article: Cesar E. P. Villegas and Alexandre R. Rocha 2020 *J. Phys.: Conf. Ser.* **1558** 012002

Journal of Physics: Conference Series **1558** (2020) 012002 doi:10.1088/1742-6596/1558/1/012002

First-principles calculation of hot carriers in black phosphorus

Cesar E. P. Villegas
Departamento de Ciencias, Universidad Privada del Norte, Lima 15314, Peru

Alexandre R. Rocha
Instituto de Física Teórica, Universidade Estadual Paulista (UNESP), Rua Dr. Bento T. Ferraz, 271, São Paulo, SP 01140-070, Brazil

E-mail: cesarperezvillegas@gmail.com

Abstract. Black Phosphorus (BP), a layered semiconductor, has atracted enormous attention due to its singular anisotropic electronic, optical and thickness-dependent direct bandgap properties. As a consequence, BP has been envisioned as a promising material for several technological applications including photonics electronics and optolectronics. Nonetheless, most of the materials that integrate these devices undergo scattering and decay processes that are governed by quantum mechanical effects. From this point of view, the correct understanding and prediction of hot carriers dynamics in prospective materials as BP is crucial for its succesfull integration in future technology. In this work, based on *ab initio* calculations, we study the carrier relaxation rates in BP. Thus, the electron-electron and electron-phonon scattering contributions are investigated. Our results suggest that for the near-infrared and visible light spectrum [1.5 to 3.5 eV], the carriers in BP follow an ultrafast dynamics with relaxation times of the order of few to tens of femtoseconds while for the far-infrared range the relaxation times is of the order of hundreds of femtoseconds. Our reults are consistent with previous studies of pump-probe measurements on carrier dynamics.

1. Introduction

Black phosphorus (BP) is a layered puckered semiconductor that has drawn renewed attention due to its strong anisotropic physical properties along its in-plane directions[1–10] and thickness-dependent energy gap, covering up from the infrared to visible electromagnetic spectrum[11, 12]. Due to these peculiar properties, the possibility of integrating BP in the design of novel optoelectronics and photonic devices [13–15] has been rapidly envisioned.

Indeed, the design of photonic devices is one of the most promising fields from the technological point of view. Since these devices rely on the controlled manipulation of photons, and its subsequent output signal detection, a correct understanding of the scattering mechanisms within a device is crucial. In fact, under external photon sources, most bulk and nanoscale materials undergo scattering and decay processes (energy loss mechanisms) that might hamper their prospective applications in electronics and optoelectronics [16]. For instance, when a nanostructure absorbs light, energetic carriers (hot carriers) are generated and rapidly thermalize to the edges of the band gap realeasing energy as heat throughout the lattice [17].

Experimentally, it is challenging to characterized the energy loss due to thermalization of hot carriers because of their fast subpicosecond lifetimes which are typically dominated by the electron-phonon and electron-electron scattering processes. In effect, ultrafast spectroscopy has been widely used to study hot carriers dynamics, although its modelling rely on model fit approaches that lack of atomistic details. Moreover, the current advances in *ab initio* modeling based on many-body perturbation theory allows an accurate description of hot carriers without the need of any empirical parameters [17, 18].

Hot carriers dynamics in BP have been vastly investigated experimentally by means of pump-probe measurements and for a wide frequency range for light pulses which yielded electron relaxation times ranging from tens to thousand of femtoseconds [19–21] as well as slightly direction-depedent hot carrier relaxation times [19].

Despite the vast literature addressing the carrier dynamics mechanisms in BP, there is still a lack of quantum mechanical approaches that accurately predicts the hot carriers dynamics in BP. In this context, here we employ many-body *ab initio* calculations to provide a theoretical description of hot carriers in BP. To this aim, both, the electron-phonon and electron-electron scattering rates are computed. Our results indicate that for the near-infrared and visible spectrum [1.5 to 3.5 eV], the carriers in BP follow an ultrafast dynamics with relaxation times of the order of few to tens of femtoseconds while for the far-infrared range, hundreds of femtoseconds can be reached.

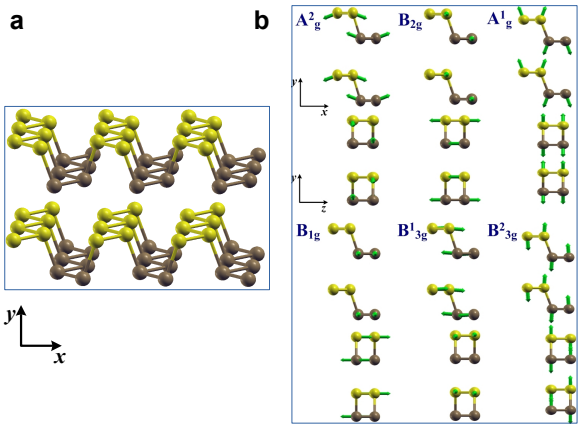

Figure 1. Schematic representation of (a) black phosphorus crystaline lattice (b) vibrational modes in black phosphorus. Only three vibrational modes are active: $A_g^2 = 463cm^{-1}$, $B_{2g} = 436cm^{-1}$, and $A_g^1 = 360cm^{-1}$ [5].

2. Methodology

We consider a pristine BP crystal, as shown in Fig. (1-a), which consists of a layered puckered structure containing 4 atoms per unit cell. The obtained fully relaxed lattice parameters (a=4.55 Å, b=3.30 Å, and c=11.28 Å) are in good agreement with those previously reported [11]. It should be notice that BP possesses 8 vibrational modes, shown in Fig. (1-b), from which only the $A_g^2 = 463cm^{-1}$, $B_{2g} = 436cm^{-1}$, and $A_g^1 = 360cm^{-1}$ correspond to active modes [5]. Thus, the optical phonon energy for BP is associated to A_g^2 which correspond $\sim$ 57 meV.

Our study is carried out following three steps. First, plane-wave density functional theory is employed to compute the electronic ground-state. The Perdue-Burke-Ernzerhof (PBE) exchange-correlation potential including van der Waals corrections within the semi-empirical dispersion scheme (PBE-D) is used. Norm-conserving pseudopotentials, along with a 80 Ry

kinetic energy cutoff and a k-sampling grid in the Monkhorst-Pack scheme of 6×8×3 as implemented in the Quantum-Espresso code.[22] The structures were fully optimized to their equilibrium position with forces smaller than 0.002 eV/Å.

Next, density functional perturbation theory (DFPT)[23] is used to compute the vibrational frequencies $\omega_{\mathbf{q}\lambda}$ and the derivatives of the self-consistent Khon-Sham potential with respect to the atomic displacements, necessary to evaluate the electron-phonon coupling matrix elements. Subsequently, many-Body perturbation theory (MBPT)[24] is used to describe the electron-phonon self-energies. There, the electron-phonon interaction is treated perturbatively[25, 26] by considering the first and a second order Taylor expansion in the nuclear displacement, commonly known as the Fan and Debye-Waller (DB) terms, respectively. The corresponding interacting Green's function, whose poles define the quasiparticle excitations, can be written as

$$G_{n\mathbf{k}}(\omega,T) = [\omega - \epsilon_{n\mathbf{k}} - \Sigma^{Fan}_{n\mathbf{k}}(\omega,T) - \Sigma^{DW}_{n\mathbf{k}}(T)]^{-1}, \tag{1}$$

where $\epsilon_{n\mathbf{k}}$ is the Khon-Sham ground-state eigenenergies for frozen atoms. Σ^{Fan} is the Fan contribution

$$\Sigma^{Fan}_{n\mathbf{k}}(i\omega,T) = \sum_{n'\mathbf{q}\lambda} \frac{|g^{\mathbf{q}\lambda}_{nn'\mathbf{k}}|^2}{N}\Big[\frac{N_{\mathbf{q}\lambda}(T)+1-f_{n'\mathbf{k}-\mathbf{q}}}{i\omega-\epsilon_{n'\mathbf{k}-\mathbf{q}}-\omega_{\mathbf{q}\lambda}} + \frac{N_{\mathbf{q}\lambda}(T)+f_{n'\mathbf{k}-\mathbf{q}}}{i\omega-\epsilon_{n'\mathbf{k}-\mathbf{q}}+\omega_{\mathbf{q}\lambda}}\Big], \tag{2}$$

and Σ^{DW} is the Debye-Waller term

$$\Sigma^{DW}_{n\mathbf{k}}(T) = -\frac{1}{2}\sum_{n'\mathbf{q}\lambda}\frac{\Lambda^{\mathbf{q}\lambda}_{nn'\mathbf{k}}}{N}\Big[\frac{2N_{\mathbf{q}\lambda}(T)+1}{\epsilon_{n\mathbf{k}}-\epsilon_{n'\mathbf{k}}}\Big]. \tag{3}$$

Here $N_{\mathbf{q}\lambda}$ and $f_{n'\mathbf{k}-\mathbf{q}}$ represent the Bose-Einstein and Fermi-Dirac distribution functions, while N is the number of $\mathbf{q}$ points in the Brillouin zone. This last $\mathbf{q}$-mesh is taken randomly to better map out the phonon transferred momentum [27]. We include 400 electronic bands and 240 random $\mathbf{q}$-points (equivalent to a 10×14×5 grid) for the phonon momentum to evaluate Eq. (2) and Eq. (3). Therefore, the electron-phonon scattering rates are computed by:

$$Im\Sigma^{e-ph}_{n\mathbf{k}} = Im[\Sigma^{Fan}_{n\mathbf{k}}(\epsilon_{n\mathbf{k}},T) + \Sigma^{DW}_{n\mathbf{k}}(T)], \tag{4}$$

The electron-electron scattering rates are computed within the one-shot GW approximation. Thus, the computation of the imaginary part of the GW self-energy, $Im\Sigma^{e-e}_{n\mathbf{k}}$, requires an 10×14×5 q-point grid together with a Kinetic energy cutoff of 6 Ry and 40 empty bands for the dielectric screening. Finally, the total relaxation times are obtained as

$$\tau_{n\mathbf{k}} = \frac{\hbar}{2}[Im\Sigma^{e-ph}_{n\mathbf{k}} + Im\Sigma^{e-e}_{n\mathbf{k}}]^{-1}. \tag{5}$$

Both the electron-phonon and electron-electron rates were computed using the the Yambo code [28].

3. Results

Figure 2-(a) depicts the imaginary parts of the self-energy corresponding to the electron-electron (e-e) and electron-phonon (e-ph) contribution within the energy range from -4.5 to 4.5 eV. For energies around the conduction band maximum (CBM) the e-ph linewidths for holes are one order of magnitude greater that the e-e ones. This effect is clearly different to what is observed in Silicon, in which for the same energy range, the e-ph rates are up to three orders of magnitude greater than the e-e linewidths [17]. It should be notice that the e-e linewidths in the range

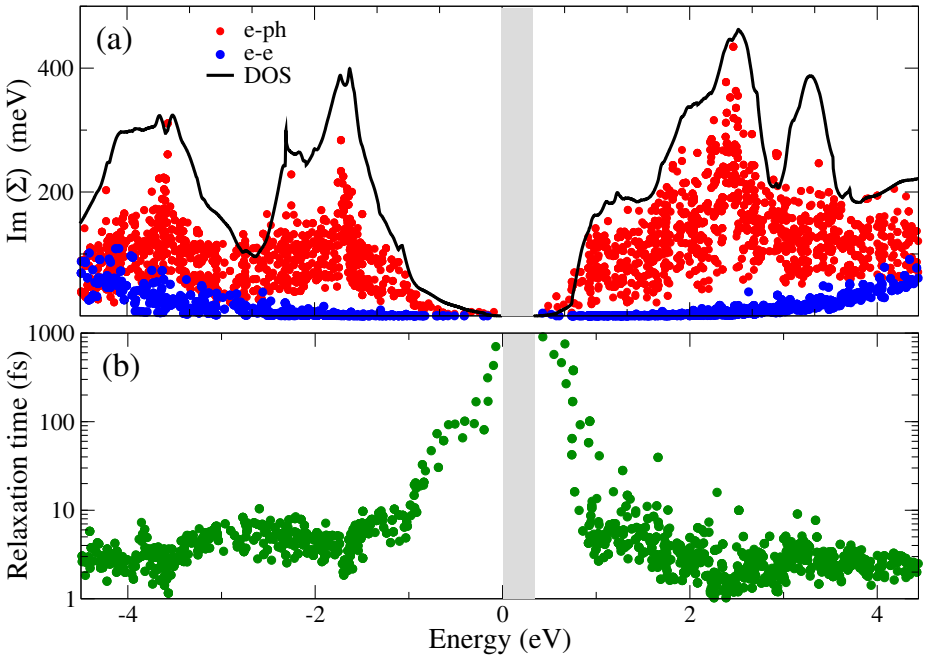

Figure 2. (a)imaginary part of the self-energy for both the electron-electron (blue dots) and electron-phonon (red dots) contributions. The solid line represents the denssity of states (DOS). (b) Total relaxation times computed though eq. (5). The shaded area indicaes the band gap of BP.

-2.0 to 2.0 eV fit very well the parabolic trend of the Keldish formula $\Gamma = \alpha(E - E_{th})^2$, where E_{th} is a energy threshold. In addition, as expected, the e-ph linewidths follow a similar trend with the density of states (DOS), since the latter represent the available phase-space of the e-ph scattering. Also, notice the strong **k** dependence of the e-ph linewidths, specially for electrons, which is reflected by the broad range of values at a fixed energy.

For the sake of completeness, in Figure 2-(b) we compute the total relaxation times by means of Eq. (5). Near the band edges, we found hot carrier relaxation times between 80-800 fs. However, 500 meV away from the band edges, faster relaxation times are observed which cover up from 5 to 80 fs. For electrons and considering the upper limit of the infrared sprectrum, $E = 1.55eV$, the relaxation rates span from 4 to 12 fs. These range of values is consistent with the experimental measurements of carrier relaxation times at photon energies of 1.5 eV [20, 21]. The results obove clearly show the ultrafast carrier relaxation in BP for the near-infrared and visible spectrum with ultrafast values as high few femtoseconds.

4. Conclusions

Using the many-body *ab initio* calculations, we have provided a theoretical description of hot carriers in BP. Our Methodology, allows the atomistic computation of the electron-phonon and electron-electron scattering rates without the need of fitting parameters. Our results suggest that for the near-infrared and visible spectrum [1.5 to 3.5 eV], the carriers in BP follow an ultrafast dynamics with relaxation times of the order of few to tens of femtoseconds while for the far-infrared range, hundreds of femtoseconds can be reached.

Acknowledgments
CEPV acknowledges the financial support from the Brazilian agency FAPESP grant number 2015/14899-0 and 2012/24227-1. A. R. R. acknowledges support from ICTP-SAIRF (FAPESP project 2011/11973-4) and the ICTP-Simons Foundation Associate Scheme. This work uses the computational resources from GRID-UNESP and CENAPAD/SP.

References

[1] Xia F, Wang H and Jia Y 2014 *Nat. Commun.* **5** 4458
[2] Qiao J, Kong X, Hu Z X, Yang F and Ji W 2014 *Nat. Commun.* **5** 4475
[3] Ling X, Wang H, Huang S, Xia F and Dresselhaus M 2015 *Proc. Natl. Acad. Sci.* **112** 4523
[4] Cakir D, Sahin H and Peeters F M 2014 *Phys. Rev. B* **90** 205421
[5] Ribeiro H B, Villegas C E P, Bahamon D A, Muraca D, Castro-Neto A H, de Souza E A T, Rocha A R, Pimenta M A and de Matos C J S 2016 *Nat. Comm.* **7** 12191
[6] Surrente A, Mitioglu A A, Galkowski K, Tabis W, Maude D K and Plochocka P 2016 *Phys. Rev. B* **93** 121405(R)
[7] Wang L, Kutana A, Zoua X and Yakobson B I 2015 *Nanoscale* **7** 9746–9751
[8] Liu T H and Chang C C 2015 *Nanoscale* **7** 10648–10654
[9] Villegas C E P, Rocha A R and Marini A 2016 *Nano Lett.* **16** 5095–5101
[10] Zhang Y Y, Pei Q X, Jiang J W, Weid N and Zhang Y W 2016 *Nanoscale* **8** 483–491
[11] Castellanos-Gomez A, Vicarelli L, Prada E, Island J O, Narasimha-Acharya K L, Blanter S I, Groenendijk D J, Buscema M, Steele G A, Alvarez J V, Zandbergen H W, Palacios J J and van der Zant H S J 2014 *2D Mater.* **1** 025001
[12] Tran V, Soklaski R, Liang Y and Yang L 2013 *Phys. Rev. B* **89** 235319
[13] Li L, Yu Y, Ye G J, Ge Q, Ou X, Wu H, Feng D, Chen X H and Zhang Y 2014 *Nat. Nanotech.* **9** 372–377
[14] Yuan H, Liu X, Afshinmanesh F, Li W, Xu G, Sun J, Lian B, Curto A G, Ye G, Hikita Y, Shen Z, Zhang S C, Chen X, Brongersma M, Hwang H Y and Cui Y 2015 *Nat. Nanotech.* **10** 707–713
[15] Miao J, Zhang L and Wang C 2019 *2D Mater.* **6** 032003
[16] Li M, Fu J, Xu Q and Sum T C 2018 *Advanced Materials* **31** 1802486
[17] Bernardi M, Vigil-Fowle D, Lischner J, Neaton J B and Louie S G 2014 *Phys. Rev. Lett.* **112** 257402
[18] Bernardi M, Vigil-Fowle D, Ong C S, Neaton J B and Louie S G 2015 *PNAS* **112** 5291–5296
[19] Ge S, Li C, Zhang Z, Zhang C L, Zhang Y, Qiu J, Wang Q, Liu J, Jia S, Feng J and Sun D 2015 *Nano Lett.* **15** 4650–4656
[20] Ge S, Li C, Zhang Z, Zhang C L, Zhang Y, Qiu J, Wang Q, Liu J, Jia S, Feng J and Sun D 2015 *Appl. Phys. Lett.* **107** 081103
[21] Wang K, Szydlowska B M, Wang G, Zhang X, Wang J J, Magan J J, Zhang L, Coleman J N, Wang J and Blau W J 2016 *ACS Nano* **10** 6923–6932
[22] Giannozzi P, Baroni S, Bonini N, Calandra M, Car R, Cavazzoni C, Ceresoli D, Cococcioni G L C M, Dabo I, Corso A D, de Gironcoli S, Fabris S, Fratesi G, Gebauer R, Gougoussis U G C, Kokalj A, Lazzeri M, Martin-Samos L, Marzari N, Mauri F, Mazzarello R, Paolini S, Pasquarello A, Paulatto L, Sbraccia C, Scandolo S, Sclauzero G, Seitsonen A P, Smogunov A, Umari P and Wentzcovitch R M 2009 *J. Phys. Condens. Matter* **21** 395502
[23] Baroni S, de Gironcoli S, Corso A D and Giannozzi P 2001 *Rev. Mod. Phys.* **73** 515–562
[24] Onida G, Reining L and Rubio A 2002 *Rev. Mod. Phys.* **74** 601–659
[25] Poncé S, Antonius G, Gillet Y, Boulanger P, Janssen J L, Marini A, Côté M and Gonze X 2014 *Phys. Rev. B.* **90** 214304
[26] Marini A, poncé S and Gonze X 2015 *Phys. Rev. B.* **91** 224310
[27] Poncé S, Antonius G, Boulanger P, Cannuccia E, Marini A, Côté M and Gonze X 2014 *physica status solidi (c)* **83** 341348
[28] Marini A, Hogan C, Grüning M and Varsano D 2009 *Computer Physics Communications* **180** 1392